

Spin-resolved correlations and ground state of a three-dimensional electron gas: Spin-polarization effects

Krishan Kumar,^{1,2} Vinayak Garg,¹ and R. K. Moudgil^{1,*}

¹*Department of Physics, Kurukshetra University, Kurukshetra-136 119, India*

²*P.G. Department of Applied Physics, S. D. College, Ambala-Cantt.-133 001, India*

(Received 2 September 2008; revised manuscript received 6 January 2009; published 6 March 2009)

We have studied the spin-resolved correlations in a three-dimensional electron gas having arbitrary spin polarization ζ by using the static and dynamical versions of the self-consistent mean-field approximation of Singwi, Tosi, Land, and Sjölander, the so-called STLS and qSTLS approaches, respectively. The spin-resolved pair-correlation functions and corresponding correlation energies, static density and spin susceptibilities, and ground-state energy are calculated over a wide range of electron number density and selected ζ . Wherever available, our results are compared directly with the recent quantum Monte Carlo studies of Ortiz *et al.* and Zong *et al.* The qSTLS approach is found to be in better agreement with the simulation data. As an interesting result, it is found that both the qSTLS and STLS methods underestimate the parallel spin-correlation energy while the antiparallel spin contribution is overestimated to the extent that the total correlation energy is in excellent agreement with the simulation data. Furthermore, a direct comparison among the results of ground-state energy at different ζ reveals, in qualitative agreement with the simulation studies, the existence of a continuous spin-polarization transition on decreasing electron density.

DOI: [10.1103/PhysRevB.79.115304](https://doi.org/10.1103/PhysRevB.79.115304)

PACS number(s): 71.10.Ca, 05.30.Fk, 71.45.Gm

I. INTRODUCTION

The homogeneous three-dimensional electron gas (3DEG) embedded in a rigid positive charge neutralizing background (the so-called jellium model) has been serving as a basic theoretical model in describing the electronic properties of metallic solids.¹ This model has also proved useful in the development of theoretical methods for materials involving inhomogeneous electron systems; for instance, it is used as input for the local density and local spin-density approximations of the density-functional theory.² At $T=0$ K, the ground state of such a 3DEG model is characterized completely by the electron number density n . To study the spin dependence of electronic ground state, it is customary to introduce spin polarization $\zeta [(n_{\uparrow}-n_{\downarrow})/n]$ as second independent parameter of the model; n_{σ} denotes the electron density for the spin component σ and $n=n_{\uparrow}+n_{\downarrow}$. In literature,³⁻⁶ the 3DEG model has been extensively studied for $\zeta=0$ within different many-body schemes over a wide coupling regime. During the last couple of years, there has been growing interest in exploring the role of ζ in determining the electronic ground state. The interest is driven mainly by the recent observation⁷ of a ferromagnetic state in lanthium doped calcium hexaboride. As an important work in this regard, Ortiz *et al.*⁸ have extended the quantum Monte Carlo (QMC) study⁹⁻¹² of the 3DEG model to include the states of arbitrary spin polarization. Among other results, it has been predicted that there occurs a continuous spin-polarization transition with decreasing electron density from the paramagnetic ($\zeta=0$) liquid to the ferromagnetic ($\zeta=1$) liquid. More precisely, the partially spin-polarized states were found to be stable in the density window $20 \pm 5 \leq r_s \leq 40 \pm 5$, with the ferromagnetic liquid becoming stable for $r_s \geq 40 \pm 5$. Here, $r_s = (4\pi n a_0^3/3)^{-1/3}$ is the usual electron-density parameter, with a_0^* being the effective Bohr radius. Owing to a weak ζ dependence of ground-state energy, Zong *et al.*¹³

have recently obtained relatively more accurate estimates for it by using diffusion QMC method (with backflow wave functions¹² and twist averaged boundary conditions¹⁴), and thereby predicted that the continuous polarization transition occurs at a much lower density $r_s \approx 50 \pm 2$, and the fully polarized phase becomes stable at the freezing density $r_s \approx 100$.

On the theory side, Bloch¹⁵ predicted a long time back an abrupt polarization transition in 3DEG at $r_s \sim 5.45$ by using the Hartree-Fock approximation (HFA). Later on, there appeared^{16,17} better estimates of ground-state energy in an attempt to incorporate correlations beyond the HFA and it was found that (i) correlations acted to increase the critical r_s for polarization transition and (ii) their inclusion beyond random-phase approximation changed an abrupt transition into a continuous one.

Until recently, only the total correlation energy of the 3DEG was known through QMC simulations. However, as an important development in the electron-gas problem, Ortiz *et al.*⁸ have also determined the QMC spin-resolved pair-correlation functions for $0.8 \leq r_s \leq 10$ at $\zeta=0$. These QMC data have been fitted accurately by Gori-Giorgi and co-workers.^{18,19} Furthermore, Gori-Giorgi and Perdew²⁰ have recently determined the spin resolution of correlation energy (into the $\uparrow\uparrow$, $\downarrow\downarrow$, and $\uparrow\downarrow$ contributions) at arbitrary ζ and r_s as an interpolation between high-density and low-density limits, consistent with the $\zeta=0$ QMC data of Ortiz *et al.*⁸ With the availability of these QMC results, it would be interesting to compare theory directly with these data, as such a comparison would be useful in judging the quality of theory in dealing with the Coulomb correlations explicitly. Davoudi *et al.*²¹ have recently determined theoretically the spin-resolved pair-correlation functions for the $\zeta=0$ and 1 states, and the results have been compared with the QMC data. However, to the best of our knowledge, theory has not yet been directly tested against the available QMC results of

spin-resolved correlation energy. Therefore, in the present work, we intend to investigate the spin-resolved correlations and related ground-state properties of the 3DEG having arbitrary ζ . Taking into consideration the reasonable success²² of the mean-field approximation of Singwi, Tosi, Land, and Sjölander (STLS) (Ref. 23) in reproducing the QMC correlation energy at $\zeta=0$, we shall employ the STLS approach to deal with the electron correlations at arbitrary ζ . We shall also incorporate correlations beyond the STLS approach by considering their dynamical nature within the mean-field approximation of Hasegawa and Shimizu²⁴—commonly referred in literature as the quantum STLS (qSTLS) approach. Wherever available, we shall compare our results with the recent QMC data.

In Sec. II, a brief account of theoretical formalism is given. In Sec. III, results and discussion are presented. We conclude our study with a brief summary in Sec. IV.

II. THEORETICAL FORMALISM

To probe the correlational properties, we make use of the dielectric formulation where the density response of the electron system to an external space-time dependent potential $V_{\sigma}^{\text{ext}}(r, t)$ plays the role of a central quantity. For an arbitrarily spin-polarized electron system, the linear density response function $\chi_{\sigma\sigma'}(q, \omega)$ is defined as²⁵

$$\rho_{\sigma}^{\text{ind}}(q, \omega) = \sum_{\sigma'} \chi_{\sigma\sigma'}(q, \omega) V_{\sigma'}^{\text{ext}}(q, \omega), \quad (1)$$

where $\rho_{\sigma}^{\text{ind}}(q, \omega)$ is the induced electron number density for the spin component σ . To determine $\rho_{\sigma}^{\text{ind}}(q, \omega)$, we use the mean-field approximation where the system of noninteracting electrons is assumed to respond to the external potential $V_{\sigma}^{\text{ext}}(q, \omega)$ plus an induced potential $V_{\sigma}^{\text{ind}}(q, \omega)$. Accordingly, $\rho_{\sigma}^{\text{ind}}(q, \omega)$ can be written as

$$\rho_{\sigma}^{\text{ind}}(q, \omega) = \chi_{\sigma}^0(q, \omega) [V_{\sigma}^{\text{ext}}(q, \omega) + V_{\sigma}^{\text{ind}}(q, \omega)], \quad (2)$$

where $\chi_{\sigma}^0(q, \omega)$ is the density response function for noninteracting electrons²⁶ having spin σ and

$$V_{\sigma}^{\text{ind}}(q, \omega) = \sum_{\sigma'} \rho_{\sigma'}^{\text{ind}}(q, \omega) V(q) [1 - G_{\sigma\sigma'}(q, \omega)]. \quad (3)$$

Here, $V(q)$ is the bare Coulomb interaction potential while $G_{\sigma\sigma'}(q, \omega)$ are the spin-resolved local-field correction (LFC) factors which represent the effect of correlations between electrons of spin σ and σ' . In the qSTLS approximation,²⁴ $G_{\sigma\sigma'}(q, \omega)$ are given as

$$G_{\sigma\sigma'}(q, \omega) = - \frac{1}{\sqrt{n_{\sigma}n_{\sigma'}}} \int \frac{d\mathbf{q}'}{(2\pi)^3} \frac{\chi_{\sigma}^0(\mathbf{q}, \mathbf{q}', \omega) V(q')}{\chi_{\sigma}^0(q, \omega) V(q)} \times [S_{\sigma\sigma'}(|\mathbf{q} - \mathbf{q}'|) - \delta_{\sigma\sigma'}], \quad (4)$$

where $S_{\sigma\sigma'}(q)$ are the spin-resolved static density structure factors and $\chi_{\sigma}^0(\mathbf{q}, \mathbf{q}', \omega)$ is the inhomogeneous noninteracting density response function²⁴ for the spin component σ . Using Eqs. (1)–(3), the density response components $\chi_{\sigma\sigma'}(q, \omega)$ are readily obtained as

$$\chi_{\sigma\sigma'}(q, \omega) = \frac{\chi_{\sigma}^0(q, \omega) [\delta_{\sigma\sigma'} + (-1)^{\delta_{\sigma\sigma'}} \psi_{\bar{\sigma}\bar{\sigma}'}(q, \omega) \chi_{\bar{\sigma}}^0(q, \omega)]}{D(q, \omega)}, \quad (5)$$

where $\bar{\sigma}$ denotes the spin orientation opposite to σ , $\psi_{\sigma\sigma'}(q, \omega) = V(q) [1 - G_{\sigma\sigma'}(q, \omega)]$ are the spin-resolved effective Coulomb potentials, and $D(q, \omega)$ is defined as

$$D(q, \omega) = [1 - \psi_{\uparrow\uparrow}(q, \omega) \chi_{\uparrow}^0(q, \omega)] [1 - \psi_{\downarrow\downarrow}(q, \omega) \chi_{\downarrow}^0(q, \omega)] - \psi_{\downarrow\uparrow}(q, \omega) \psi_{\uparrow\downarrow}(q, \omega) \chi_{\uparrow}^0(q, \omega) \chi_{\downarrow}^0(q, \omega). \quad (6)$$

However, $S_{\sigma\sigma'}(q)$ are related to $\chi_{\sigma\sigma'}(q, \omega)$ through the fluctuation-dissipation theorem¹ as

$$S_{\sigma\sigma'}(q) = - \frac{\hbar}{\pi \sqrt{n_{\sigma}n_{\sigma'}}} \int_0^{\infty} d\omega \chi_{\sigma\sigma'}(q, i\omega). \quad (7)$$

This implies that $\chi_{\sigma\sigma'}(q, \omega)$ have to be obtained numerically from the self-consistent solution of the set of Eqs. (4), (5), and (7). The ω integration in Eq. (7) is performed along the imaginary ω axis to avoid the difficulty of plasmon poles on the real ω axis.²⁷

The ground-state energy E_g (per electron), the quantity of central interest for determining the equilibrium spin polarization, is obtained in accordance with the ground-state energy theorem²⁸ as

$$E_g = \frac{1}{n} \sum_{\sigma} n_{\sigma} \frac{(6\pi n_{\sigma})^{2/3}}{2m^*} + \int_0^{e^2} d\lambda \frac{E^{\text{int}}(\lambda)}{\lambda}, \quad (8)$$

where the first term is the free-electron kinetic energy while the second term represents the potential energy (E^{pot}). $E^{\text{int}}(\lambda) = [E_{\uparrow\uparrow}^{\text{int}}(\lambda) + E_{\downarrow\downarrow}^{\text{int}}(\lambda) + E_{\uparrow\downarrow}^{\text{int}}(\lambda)]/n$ is the interaction energy per electron for a 3DEG with Coulomb coupling λ and m^* is the effective electron mass. The spin-resolved interaction energy $E_{\sigma\sigma'}^{\text{int}}(\lambda)$ is given by

$$E_{\sigma\sigma'}^{\text{int}}(\lambda) = \frac{\sqrt{n_{\sigma}n_{\sigma'}}}{(1 + \delta_{\sigma\sigma'})} \sum_{\mathbf{q} \neq 0} V(q) [S_{\sigma\sigma'}(q, \lambda) - \delta_{\sigma\sigma'}]. \quad (9)$$

Thus, we see that the calculation of E_g requires only the knowledge of $S_{\sigma\sigma'}(q, \lambda)$.

It is appropriate to mention here that one can obtain the corresponding STLS formalism simply by replacing the above $G_{\sigma\sigma'}(q, \omega)$ by their behavior in the limit, $\hbar \rightarrow 0$, wherein they become static and are given as

$$G_{\sigma\sigma'}(q) = - \frac{1}{\sqrt{n_{\sigma}n_{\sigma'}}} \int \frac{d\mathbf{q}'}{(2\pi)^3} \frac{\mathbf{q} \cdot \mathbf{q}'}{q'^2} [S_{\sigma\sigma'}(|\mathbf{q} - \mathbf{q}'|) - \delta_{\sigma\sigma'}]. \quad (10)$$

Furthermore, we wish to point out that in the qSTLS approach, $G_{\uparrow\downarrow}(q, \omega) \neq G_{\downarrow\uparrow}(q, \omega)$. This asymmetry of the LFC factor, which arises directly from the factor $[\chi_{\sigma}^0(\mathbf{q}, \mathbf{q}', \omega)/\chi_{\sigma}^0(q, \omega)]$ in Eq. (4), would in turn lead to an asymmetric $\chi_{\sigma\sigma'}(q, \omega)$. However, $\chi_{\sigma\sigma'}(q, \omega)$ must be symmetric under an interchange in spin index. We overcome this problem by taking the antiparallel spin LFC factor as an average of $G_{\uparrow\downarrow}(q, \omega)$ and $G_{\downarrow\uparrow}(q, \omega)$. However, there is no such problem with the STLS $G_{\uparrow\downarrow}(q)$.

III. RESULTS AND DISCUSSION

Throughout the numerical results presented, lengths are in units of the inverse up-spin Fermi wave vector $(k_{F\uparrow})^{-1}$, energies in units of effective Rydberg [$1 \text{ Ry}^* = e^2/(2a_0^*)$], and $\hbar = 1$. We begin with the discussion of spin-resolved correlation functions.

A. Spin-resolved correlation functions

Equations (4), (5), and (7) are solved numerically in an iterative manner for $S_{\uparrow\uparrow}(q)$, $S_{\downarrow\downarrow}(q)$, and $S_{\uparrow\downarrow}(q)$, and the solution was accepted when the convergence in $G_{\uparrow\uparrow}(q, \omega)$, $G_{\downarrow\downarrow}(q, \omega)$, and $G_{\uparrow\downarrow}(q, \omega)$ (at each of the q and ω values) was better than 0.0001%. However, it became almost impossible to find the self-consistent solution at and above a critical r_s , say r_s^c ; for instance, $r_s^c \approx 7$ at $\zeta=0$. The value of r_s^c was seen to decrease gradually with increasing ζ . An analysis of the numerical calculation reveals that the problem of non-converging $G_{\sigma\sigma'}(q, \omega)$ is related to the emergence of poles in $\chi_{\sigma\sigma'}(q, \omega)$ at a finite ω [say $\omega_0(q)$] over a definite q interval, $0 \leq q \leq q_c$. A similar kind of numerical instability was earlier identified by Moudgil *et al.*²⁹ in a two-dimensional electron gas. Obviously, the presence of poles in $\chi_{\sigma\sigma'}(q, \omega)$ constitutes an unphysical result because such poles imply an excitation of the system at imaginary frequencies. However, we find concurrently that the ‘‘direct calculation’’ of total charge-charge (CC) structure factor $S_{CC}(q)$, which is possible only at $\zeta=0$ and 1, does not exhibit any poles, and therefore, the self-consistent $S_{CC}(q)$ can be determined for r_s beyond r_s^c . In the direct calculation, $S_{CC}(q)$ is obtained through the computation of total CC density response function, $\chi_{CC}(q, \omega) = \sum_{\sigma\sigma'} \chi_{\sigma\sigma'}(q, \omega)$, whose calculation at $\zeta=0$ and 1 involves only one independent LFC factor. Naturally, $S_{CC}(q)$ obtained from the direct calculation must match (at any r_s) with the one determined through the self-consistent $\chi_{\sigma\sigma'}(q, \omega)$. In terms of its components, $S_{CC}(q)$ is given as

$$S_{CC}(q) = \frac{1+\zeta}{2} S_{\uparrow\uparrow}(q) + \frac{1-\zeta}{2} S_{\downarrow\downarrow}(q) + \sqrt{1-\zeta^2} S_{\uparrow\downarrow}(q).$$

This relation, in turn, suggests that there must occur, for $r_s \geq r_s^c$, some sort of cancellation among the (singular) response functions $\chi_{\uparrow\uparrow}(q, \omega)$, $\chi_{\downarrow\downarrow}(q, \omega)$, and $\chi_{\uparrow\downarrow}(q, \omega)$ so as to have a nonsingular $\chi_{CC}(q, \omega)$. Keeping this point in mind, we make an attempt to handle the problem of poles in $\chi_{\sigma\sigma'}(q, \omega)$ in a purely mathematical sense. We may mention that the poles of $\chi_{\sigma\sigma'}(q, \omega)$ can only be located numerically. Taking into account the existence of a pole at $\omega = \omega_0(q)$ on the imaginary ω axis, it is straightforward to show³⁰ that Eq. (7) gets modified as

$$S_{\sigma\sigma'}(q) = -\frac{1}{\pi \sqrt{n_{\sigma} n_{\sigma'}}} \int_0^{\infty} d\omega \left[\chi_{\sigma\sigma'}(q, \omega) - \frac{a_{\sigma\sigma'}}{\omega - \omega_0(q)} + \frac{a_{\sigma\sigma'}}{\omega + \omega_0(q)} \right]. \quad (11)$$

Here, $a_{\sigma\sigma'} = [\chi_{\sigma\sigma'}(q, \omega_0) D(q, \omega_0)] / D'(q, \omega_0)$ is the first-order residue of $\chi_{\sigma\sigma'}(q, \omega)$ at $\omega = \omega_0(q)$, with $D'(q, \omega_0)$ be-

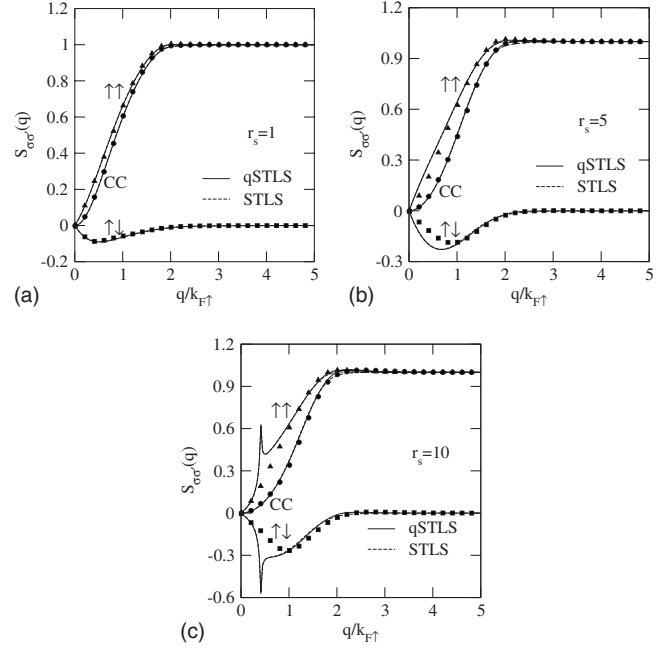


FIG. 1. The spin-resolved structure factors $S_{\sigma\sigma'}(q)$ vs $q/k_{F\uparrow}$ for $\zeta=0$ at indicated r_s . The curve marked ‘‘CC’’ is the total charge-charge structure factor $S_{CC}(q)$. The symbols \blacktriangle , \blacksquare , and \bullet represent, respectively, the QMC data of Ortiz *et al.* (taken from Ref. 18) for $S_{\uparrow\uparrow}(q)$, $S_{\uparrow\downarrow}(q)$, and $S_{CC}(q)$.

ing the first derivative of $D(q, \omega)$ at $\omega = \omega_0(q)$. Using the modified $S_{\sigma\sigma'}(q)$ [viz. Eq. (11)], we were able to find the self-consistent solution for r_s beyond r_s^c . As an important check on the accuracy of our method for dealing with poles, we found that $S_{CC}(q)$ obtained through the self-consistent $S_{\sigma\sigma'}(q)$ and that via the direct calculation of $\chi_{CC}(q, \omega)$ matched perfectly within the convergence tolerance. In the STLS calculation too, $\chi_{\sigma\sigma'}(q, \omega)$ exhibits similar kind of poles and these are treated by using the procedure as given above.

We depict in Figs. 1(a)–1(c) the self-consistent $S_{\sigma\sigma'}(q)$ at $\zeta=0$, viz. $S_{\uparrow\uparrow}(q)$ [= $S_{\downarrow\downarrow}(q)$] and $S_{\uparrow\downarrow}(q)$, for $r_s=1, 5$, and 10 in both the qSTLS and STLS approaches. The resulting total CC structure factor $S_{CC}(q)$ [i.e., the one computed from the self-consistent $S_{\sigma\sigma'}(q)$] is also shown. For direct comparison, the QMC data of Ortiz *et al.*⁸ (as fitted by Gori-Giorgi *et al.*¹⁸) is shown by symbols. At low r_s , both the qSTLS and STLS results are in very good agreement with the QMC data. However, the extent of agreement somewhat begins diminishing with increasing r_s . Apart from this quantitative difference, both the qSTLS and STLS theories predict, in complete contrast with the QMC results, a sharp peak in $S_{\sigma\sigma'}(q)$ at $r_s=10$. In contrast, the corresponding $S_{CC}(q)$ remains a smooth function of q , and in fact, it is in very good agreement with the QMC data [see Fig. 1(c)]. This feature of $S_{CC}(q)$ clearly demonstrates that there is a perfect cancellation between the peaks in $S_{\uparrow\uparrow}(q)$ and $S_{\uparrow\downarrow}(q)$. Furthermore, we detect that the appearance of a spurious peak in $S_{\sigma\sigma'}(q)$ at $r_s=10$ has its direct relation with the evolution of poles in $\chi_{\sigma\sigma'}(q, \omega)$. In fact, $S_{\sigma\sigma'}(q)$ starts exhibiting this kind of peak for $r_s > r_s^c$ itself. To elaborate this relationship, we have plotted in Fig. 2 the qSTLS results of $\omega_0(q)$ for $\zeta=0$ and 0.2

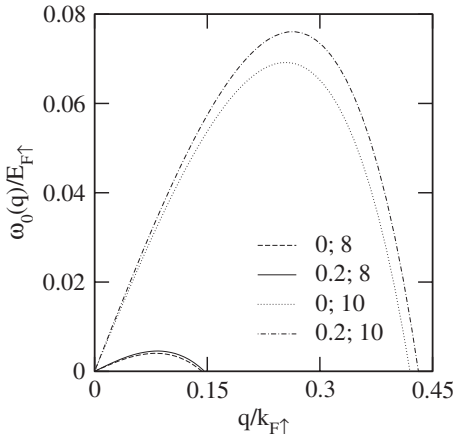


FIG. 2. The pole position $\omega_0(q)/E_{F\uparrow}$ vs $q/k_{F\uparrow}$ at selected ζ and r_s in the qSTLS approach. The pair of legends represent, respectively, the values of ζ and r_s ; $E_{F\uparrow}$ denotes the Fermi energy for the \uparrow spin electrons.

at $r_s=8$ and 10. Apparently, $\chi_{\sigma\sigma'}(q, \omega)$ has poles over a definite q interval $0 \leq q \leq q_c$, and this interval widens with increasing r_s (ζ) at a given ζ (r_s). Particularly, we wish to point out that both q_c and $\omega_0(q_c)$ tend to zero for $r_s \rightarrow r_s^c$ at a given ζ . It can also be noted from Figs. 1(c) and 2 that $S_{\sigma\sigma'}(q)$ has peak exactly at $q=q_c$. Qualitatively similar kind of behavior of $\omega_0(q)$ is found in the STLS approach. Although not reported here, $S_{\sigma\sigma'}(q)$ and $S_{CC}(q)$ are seen to have a similar r_s dependence at nonzero ζ also.

Above results on $S_{\sigma\sigma'}(q)$ and $S_{CC}(q)$ seem to imply that, while the qSTLS and STLS theories fail completely in handling the spin-resolved correlations for $r_s > r_s^c$, they still yield a fairly good account of the spin-averaged correlations. Nevertheless, our study explicates the mechanism which leads to the eventual failure of these theories in treating the spin-resolved correlations for $r_s > r_s^c$.

Next, we compute the spin-resolved pair-correlation functions $g_{\sigma\sigma'}(r)$ by taking the inverse Fourier transform of self-consistent $S_{\sigma\sigma'}(q)$. Figures 3(a)–3(c) contain the numerical results of $g_{\uparrow\uparrow}(r)$, $g_{\uparrow\downarrow}(r)$, and the spin-averaged correlation function $g(r) = [g_{\uparrow\uparrow}(r) + g_{\uparrow\downarrow}(r)]/2$ at $\zeta=0$ for $r_s=1, 5$, and 10 in both the qSTLS and STLS approaches. The QMC results of Ortiz *et al.*⁸ (as fitted by Gori-Giorgi *et al.*¹⁸) are shown by symbols. Quite generally, it is noted that the qSTLS results of both $g_{\sigma\sigma'}(r)$ and $g(r)$ compare more favorably with the QMC data. Improvement over the STLS predictions is seen to become increasingly visible, particularly at small r , with the increasing r_s . Among notable features, the qSTLS results satisfy the condition of positive definiteness except for the little negative behavior of $g_{\uparrow\uparrow}(r)$ at small r for low r_s (≤ 3). In contrast, the STLS $g_{\uparrow\uparrow}(r)$ remains negative at small r over the r_s range shown and, in addition, even $g(r)$ and $g_{\uparrow\downarrow}(r)$ start assuming negative values at small r for $r_s \geq 5$. The better quality of the qSTLS results is attributed to the inclusion of the dynamics of correlations through a frequency-dependent LFC factor.

In Fig. 4, we illustrate the ζ dependence of $g_{\sigma\sigma'}(r)$ in the qSTLS approach at $r_s=4$ —a value smaller than r_s^c for the depicted ζ . Evidently, $g_{\downarrow\downarrow}(r)$ and $g_{\uparrow\downarrow}(r)$ are relatively more

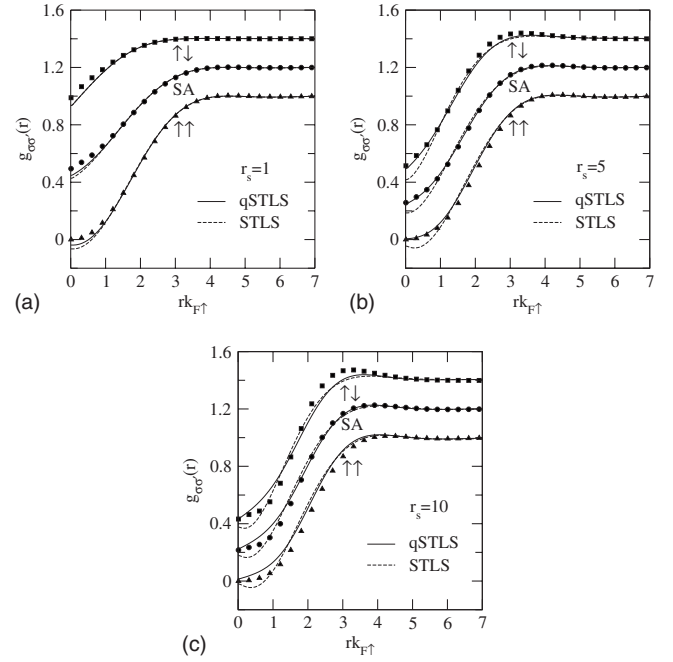


FIG. 3. The spin-resolved pair-correlation functions $g_{\sigma\sigma'}(r)$ vs $rk_{F\uparrow}$ for $\zeta=0$ at indicated r_s . The curves are labeled in the same way as in Fig. 1. For clarity, the results of spin-averaged pair-correlation function $g(r)$ (marked as “SA”), and $g_{\uparrow\downarrow}(r)$ have been shifted vertically by 0.2 and 0.4, respectively.

sensitive to ζ . At first sight, it may appear that $g_{\uparrow\downarrow}(r)$ should not depend on ζ at constant r_s as it represents correlations due to the Coulomb coupling among electrons. Actually, with increasing ζ , the kinetic energy for the minority-spin (\downarrow) component comes down while it goes up for the majority-spin (\uparrow) component. As a result, the \downarrow spin electrons become more correlated than the \uparrow spin electrons. In turn, this directly affects the $\uparrow\downarrow$ correlations even though r_s remains constant. This simple-minded picture explains the ζ dependence of $g_{\sigma\sigma'}(r)$. To the best of our knowledge, the QMC results of $g_{\sigma\sigma'}(r)$ are not available for $0 < \zeta < 1$.

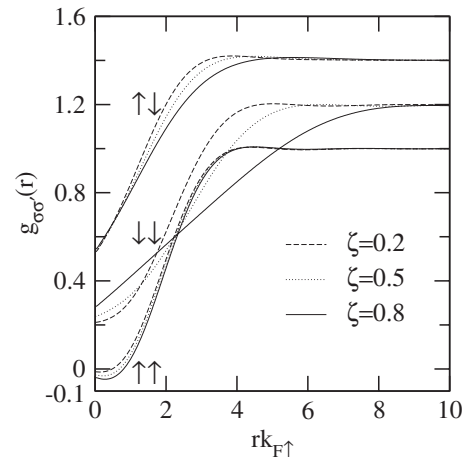


FIG. 4. The spin-resolved pair-correlation functions $g_{\sigma\sigma'}(r)$ vs $rk_{F\uparrow}$ for $r_s=4$ at indicated ζ in the qSTLS approach. For clarity, the curves of $g_{\downarrow\downarrow}(r)$ and $g_{\uparrow\downarrow}(r)$ have been shifted vertically by 0.2 and 0.4, respectively.

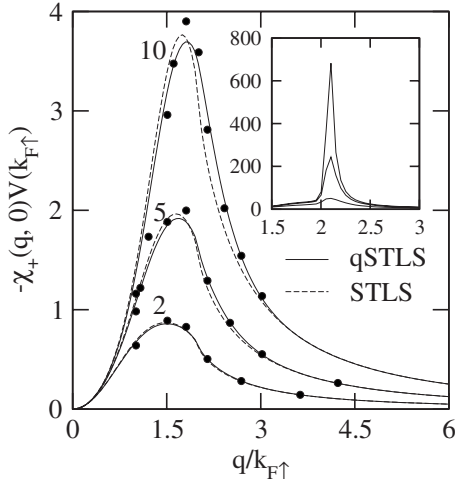


FIG. 5. The static density susceptibility $[-\chi_+(q,0)V(k_{F\uparrow})]$ vs $q/k_{F\uparrow}$ for $\zeta=0$ at different r_s . The legends indicate the r_s parameter. The symbols are the QMC results taken from Ref. 31. The inset depicts the static density susceptibility at $r_s=50, 75,$ and 84.9 , in the order of increasing peak height.

B. Static susceptibility and local fields

For having further insight into the behavior of electrons near the instability ($r_s \sim r_s^c$), we calculate the static (i.e., $\omega=0$) susceptibility $\chi(q,0)$, which can be obtained by diagonalizing the density response matrix as

$$\chi_{\pm}(q,0) = \frac{2\chi_{\uparrow}(q,0)\chi_{\downarrow}(q,0)}{D_1(q) \pm \sqrt{D_2(q)}}, \quad (12)$$

where $D_1(q) = \chi_{\uparrow}(q,0) + \chi_{\downarrow}(q,0)$, $D_2(q) = [\chi_{\downarrow}(q,0) - \chi_{\uparrow}(q,0)]^2 + 4\{\psi_{\uparrow\downarrow}(q,0)\chi_{\uparrow}(q,0)\chi_{\downarrow}(q,0)\}^2$, and $\chi_{\sigma}(q,0)$ is defined as

$$\chi_{\sigma}(q,0) = \frac{\chi_{\sigma}^0(q,0)}{1 - \psi_{\sigma\sigma}(q,0)\chi_{\sigma}^0(q,0)}.$$

In Eq. (12), the “+” and “−” signs correspond, respectively, to the in-phase and out-of-phase (π) modes of $\rho_{\uparrow}^{\text{ind}}(q,0)$ and $\rho_{\downarrow}^{\text{ind}}(q,0)$. Equivalently, $\chi_+(q,0)$ is the static density susceptibility while $\chi_-(q,0)$ the static spin susceptibility. The numerical results of $\chi_+(q,0)$ and $\chi_-(q,0)$ at $\zeta=0$ are given, respectively, in Figs. 5 and 6 at selected r_s . $\chi_+(q,0)$ is also compared with the available QMC data due to Moroni *et al.*³¹ and the STLS results. Once again, we note that the qSTLS predictions are in better agreement with the QMC data. On the other hand, the QMC study is not available for $\chi_-(q,0)$. However, both the qSTLS and STLS calculations reveal that $\chi_-(q,0)$ enhances with increasing r_s and prominently, the $\lim_{q \rightarrow 0} \chi_-(q,0)$ is found to diverge at $r_s \approx r_s^c$, which indicates the existence of a spin-polarization transition at $r_s \approx r_s^c$. Unlike the earlier STLS (Ref. 32) and qSTLS (Ref. 33) studies on the 3DEG, we could see $\chi_-(q,0)$ actually diverging due to the availability of self-consistent $G_{\sigma\sigma'}(q,\omega)$ at any desired r_s . It may be recapitulated that r_s^c is the critical r_s at which $\chi_{\sigma\sigma'}(q,\omega)$ exhibits poles for the first time, and that, at r_s^c , q_c and $\omega_0(q_c) \rightarrow 0$. Noting that $\chi_-(q,0) \propto [\rho_{\uparrow}^{\text{ind}}(q,0) - \rho_{\downarrow}^{\text{ind}}(q,0)]$, the divergence of $\lim_{q \rightarrow 0} \chi_-(q,0)$

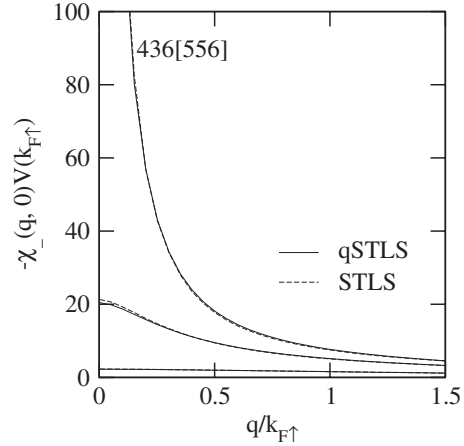


FIG. 6. The static spin susceptibility $[-\chi_-(q,0)V(k_{F\uparrow})]$ vs $q/k_{F\uparrow}$ for $\zeta=0$ at $r_s=2, 5,$ and 6.8 . The curves from bottom to top are in the order of increasing r_s . The numbers near the topmost curve represent the value of spin susceptibility in the limit $q \rightarrow 0$ in the qSTLS (STLS) approximation.

simply reflects the emergence of pole in $\chi_{\sigma\sigma'}(q,\omega)$ at $r_s = r_s^c$.

On the contrary, $\chi_+(q,0)$ remains finite at $r_s = r_s^c$. This is expected too as $\chi_+(q,0) \propto [\rho_{\uparrow}^{\text{ind}}(q,0) + \rho_{\downarrow}^{\text{ind}}(q,0)]$, and there occurs a perfect cancellation between the diverging $\rho_{\uparrow}^{\text{ind}}(q,0)$ and $\rho_{\downarrow}^{\text{ind}}(q,0)$. However, we find that the peaked structure in the qSTLS $\chi_+(q,0)$ grows monotonically with r_s , and it is eventually seen to diverge at $q/k_{F\uparrow} \approx 2.1$, for $r_s \approx 85$ (see the inset of Fig. 5). This divergence in $\chi_+(q,0)$ may be interpreted as a precursor of the occurrence of a liquid-Wigner crystal³⁴ phase transition. Interestingly, the predicted crystallization density lies close to its recent QMC estimate ($r_s \sim 100$) by Zong *et al.*¹³ However, the STLS $\chi_+(q,0)$ does not show any divergence. As can be seen from Eq. (12) and Fig. 7, the difference between the qSTLS and STLS predictions arises entirely due to different behavior of the (static) LFC

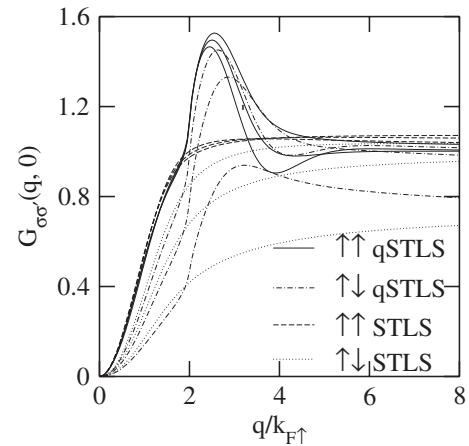


FIG. 7. Comparison between the qSTLS and STLS spin-resolved static LFCs at $\zeta=0$ for $r_s=2, 5,$ and 10 . In case of the $\uparrow\downarrow$ LFCs, the curves from bottom to top are in the order of increasing r_s . For the qSTLS $G_{\uparrow\uparrow}(q,0)$, curves in the order of decreasing peak height (at $q/k_{F\uparrow} \sim 2.5$) are for increasing r_s while the STLS $G_{\uparrow\uparrow}(q)$ depends mildly on r_s .

TABLE I. The ground-state energy $E_g(r_s, \zeta)$ (in Ry^*/e) at some representative values of r_s and ζ in different schemes. STLS and qSTLS from present calculations, OHB/QMC from Ortiz, Harris, and Ballone (Ref. 8), ZLC/QMC from Zong, Lin, and Ceperley (Ref. 13), and DAPT from Davoudi, Asgari, Polini, and Tosi (Ref. 21).

r_s	Different calculations	$\zeta=0.0$	$\zeta=0.2$	$\zeta=0.333$	$\zeta=0.667$	$\zeta=0.8$	$\zeta=1.0$
10.0	OHB/QMC	-0.106					-0.101
	DAPT	-0.10562		-0.10488	-0.10277		-0.09957
	STLS	-0.10585	-0.10571	-0.10546	-0.10425	-0.10351	-0.10198
	qSTLS	-0.1050	-0.1049	-0.1046	-0.1036	-0.1030	-0.1015
13.0	qSTLS	-0.0868	-0.0868	-0.0869	-0.0868	-0.0865	-0.0857
13.5	qSTLS	-0.0844	-0.0844	-0.0844	-0.0845	-0.0843	-0.0835
17.4	STLS	-0.06983	-0.06984	-0.06984	-0.06979	-0.06974	-0.06955
18.5	STLS	-0.06645	-0.06645	-0.06646	-0.06647	-0.06644	-0.06631
20.0	OHB/QMC	-0.063					-0.0625
	DAPT	-0.06265		-0.06250	-0.06210		-0.06153
	STLS	-0.06233	-0.06234	-0.06236	-0.06240	-0.06240	-0.06232
	qSTLS	-0.0616	-0.0617	-0.0619	-0.0624	-0.623	-0.0619
24.4	STLS	-0.05274	-0.05276	-0.05279	-0.05291	-0.05294	-0.05295
40.0	ZLC/QMC	-0.035 237 48(60)		-0.035 232 95(67)	-0.035 205 39(67)		-0.035 134 83(72)
	DAPT	-0.03470		-0.03467	-0.03459		-0.03450
	STLS	-0.03422	-0.03423	-0.03427	-0.03439	-0.03444	-0.03450
	qSTLS	-0.0336	-0.0338	-0.0340	-0.0344	-0.0344	-0.0342
50.0	ZLC/QMC	-0.028 899 00(62)		-0.028 899 62(68)	-0.028 888 35(62)		-0.028 849 83(81)
	OHB/QMC	-0.029					-0.0288
	DAPT	-0.02845		-0.02844	-0.02839		-0.02834
	STLS	-0.02797	-0.02798	-0.02801	-0.02812	-0.02816	-0.02821
	qSTLS	-0.0275	-0.0276	-0.0277	-0.0281	-0.0281	-0.0279
70.0	ZLC/QMC	-0.021 314 29(41)		-0.021 316 21(39)	-0.021 315 93(37)		-0.021 306 67(37)
	qSTLS	-0.0201	-0.0202	-0.0203	-0.0205	-0.0205	-0.0205

factors in the two theories. Furthermore, the ζ dependence of $\chi_{\pm}(q, 0)$ (although not reported here) implies that the critical r_s , at which $\chi_{\pm}(q, 0)$ shows divergence, is greatly reduced at finite ζ . This seems to suggest that the partially spin-polarized 3DEG may exhibit the magnetic or structural instabilities at relatively lower r_s values.

C. Ground-state energy

Equation (8) can be recasted to obtain the ground-state energy (per electron) in reduced units as

$$E_g(r_s, \zeta) = \frac{3}{10r_s^2} \left(\frac{9\pi}{4} \right)^{2/3} [(1+\zeta)^{5/3} + (1-\zeta)^{5/3}] + C \int_0^{r_s} dr'_s \int_0^{\infty} dq [S_{CC}(q, r'_s, \zeta) - 1], \quad (13)$$

where $C = [2/(\pi r_s^2)][9\pi(1+\zeta)/4]^{1/3}$. As discussed in Sec. III A, although our results of $S_{\sigma\sigma'}(q)$ are not reliable for $r_s > r_s^c$, the resulting $S_{CC}(q)$ shows a good agreement with the available QMC data. Since the computation of E_g depends entirely on $S_{CC}(q)$, we believe that our calculation of E_g should be reliable also for $r_s > r_s^c$. Table I contains our results of E_g at some representative values of r_s and ζ , along with

the available QMC data^{8,13} and the results of Davoudi *et al.*²¹ Importantly, E_g depends weakly on ζ and therefore, the energy calculation demands high numerical accuracy to be able to predict any polarization transition. To this endeavor, we have tested comprehensively the accuracy of our results of E_g , and the error (in Ry^*) is of the order of 10^{-6} and 10^{-5} in the STLS and qSTLS calculations, respectively. It is evident from Table I that both the STLS and qSTLS theories predict, in qualitative agreement with the QMC studies, a continuous spin-polarization transition with increasing r_s . Particularly, the STLS theory shows that the ground state is paramagnetic for $r_s \lesssim 17$ and the partially spin-polarized phases emerge stable in the density window $17 \lesssim r_s \lesssim 24$, with the fully polarized phase becoming stable for $r_s \gtrsim 24.4$ (see Fig. 8). Apparently, the STLS predictions are closer to the QMC study of Ortiz *et al.*⁸ On the other hand, the qSTLS theory predicts that the polarization transition sets in at $r_s \approx 13$. Initially, the equilibrium polarization increases quite fast with r_s but then it stays nearly constant at $\zeta \sim 0.8$ for $20 \lesssim r_s \lesssim 65$. At $r_s \approx 70$, the energies of the $\zeta=0.667$, 0.8, and 1 states become equal within the numerical accuracy. Clearly, higher accuracy is needed to resolve the relative stability of these states. However, the emergence of poles in $\chi_{\sigma\sigma'}(q, \omega)$ for $r_s \geq r_s^c$ does not allow a better accuracy of $E_g(r_s, \zeta)$. Nevertheless, it is gratifying to note that the qSTLS critical density for

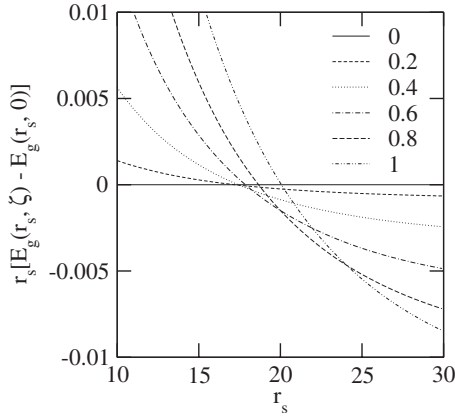


FIG. 8. The spin-polarization energy (in Ry^*/e) times r_s , i.e., $r_s[E_g(r_s, \zeta) - E_g(r_s, 0)]$ vs r_s at different ζ in the STLS approach. The legends represent the values of ζ .

(nearly) full polarization is much closer to the QMC study of Zong *et al.*¹³ Furthermore, it is seen from Table I that the present results are in good agreement with the QMC data and the results of Davoudi *et al.*²¹ at low r_s . However, the agreement somewhat diminishes with increasing r_s , and the results of Davoudi *et al.*²¹ remain relatively closer to the QMC data. Furthermore, we note that the spin susceptibility and ground-state energy calculations reveal polarization transition at markedly different r_s . This mismatch reflects the violation of the spin-susceptibility sum rule^{32,33} and it constitutes a known drawback of the qSTLS and STLS approaches.

D. Spin-resolved correlation energy

The total correlation energy $E^c(r_s, \zeta)$ can be decomposed into the $\uparrow\uparrow$, $\downarrow\downarrow$, and $\uparrow\downarrow$ contributions as

$$E^c(r_s, \zeta) = E_{\uparrow\uparrow}^c(r_s, \zeta) + E_{\downarrow\downarrow}^c(r_s, \zeta) + E_{\uparrow\downarrow}^c(r_s, \zeta). \quad (14)$$

$E_{\sigma\sigma'}^c$ is obtained by subtracting the exchange energy, $E_{\sigma\sigma'}^{\text{ex}} = -(3\delta_{\sigma\sigma'}/4\pi r_s)(9\pi/4)^{1/3}[1 + (-1)^{\delta_{\sigma\downarrow}}\zeta]^{4/3}$, from the corresponding potential energy $E_{\sigma\sigma'}^{\text{pot}}$. The numerical results of $E_{\sigma\sigma'}^c(r_s, \zeta)$ and the resultant $E^c(r_s, \zeta)$ are given in Figs. 9(a)–9(c) at selected ζ , along with the available QMC results, as fitted analytically by Gori-Giorgi and Perdew.²⁰ Notably, both the qSTLS and STLS approaches somewhat underestimate the $\uparrow\uparrow$ and $\downarrow\downarrow$ correlation energies, whereas the $\uparrow\downarrow$ correlation energy is overestimated. Interestingly, the underestimation in the former is almost exactly canceled out by the overestimation in the latter, with the result that the total correlation energy $E^c(r_s, \zeta)$ is found to be in very good agreement with the QMC results. Furthermore, we note that the evolution of unphysical poles in $\chi_{\sigma\sigma'}(q, \omega)$ also reflects in the behavior of $E_{\sigma\sigma'}^c(r_s, \zeta)$, and our predictions of $E_{\sigma\sigma'}^c(r_s, \zeta)$ are not reliable for $r_s > r_s^c$. Therefore, we cannot testify the recent prediction of the positivelike spin-correlation energy at low density by Gori-Giorgi and Perdew.²⁰ However, the total correlation energy $E^c(r_s, \zeta)$ continues to remain well behaved and close to the QMC data for r_s much beyond r_s^c [see Fig. 9(d)]. Thus, we find that the STLS ansatz captures nicely the spin-averaged properties of the 3DEG but it is not

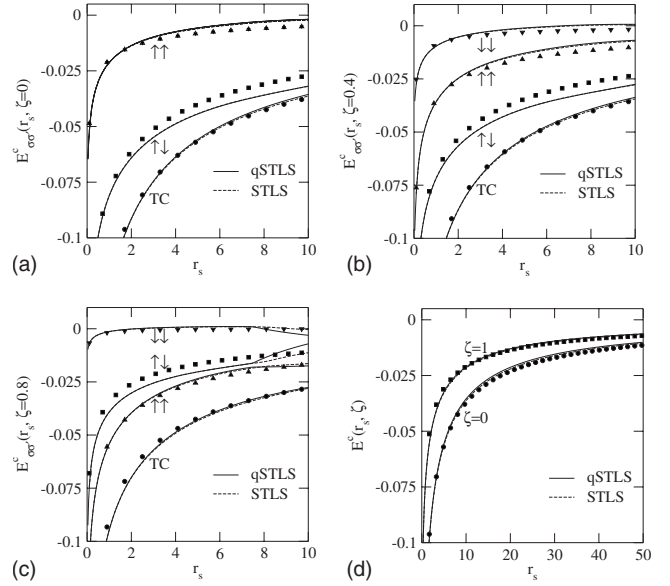


FIG. 9. [(a)–(c)] The spin-resolved correlation energy $E_{\sigma\sigma'}^c(r_s, \zeta)$ (in Ry^*/e) vs r_s at selected ζ . The curve marked “TC” is the total correlation energy. The symbols \blacktriangle , \blacktriangledown , \blacksquare , and \bullet represent, respectively, the QMC data (taken from Ref. 20) for the $\uparrow\uparrow$, $\downarrow\downarrow$, $\uparrow\downarrow$, and the total correlation energies. (d) The total correlation energy $E^c(r_s, \zeta)$ vs r_s at $\zeta=0$ and 1. The symbols are the QMC results (taken from Ref. 20).

that good in handling the spin-resolved correlations.

IV. SUMMARY AND CONCLUSIONS

In summary, we have presented a theoretical study of spin-resolved correlations in a 3DEG having arbitrary spin polarization ζ by using the STLS and qSTLS approaches. The spin-resolved pair-correlation functions and correlation energies, static density and spin susceptibilities, and ground-state energy are calculated at selected ζ over a wide range of r_s . Wherever available, our results are compared with the QMC results. Quite generally, the results of qSTLS approach are found to be in better agreement with the simulation data. In particular, the improvement over the STLS predictions has been seen to become quite prominent with the increasing value of r_s . This result clearly underlines the growing importance of the dynamical nature of correlations with increasing r_s . However, we encounter a critical r_s (namely, r_s^c) in both the STLS and qSTLS calculations, at and above which it becomes difficult to compute the self-consistent $S_{\sigma\sigma'}(q)$. As an important finding, we have resolved that this difficulty is related to the emergence of unphysical poles in $\chi_{\sigma\sigma'}(q, \omega)$ on the imaginary ω axis for $0 < q < q_c$. We have developed a purely mathematical procedure for handling these poles, using, which we were able to find, the self-consistent $S_{\sigma\sigma'}(q)$ for r_s beyond r_s^c . It turned out that, although the qSTLS and STLS approaches break down in describing the spin-resolved correlations for $r_s > r_s^c$, they provide a fairly good description of the spin-averaged correlations. Building upon this result, we have calculated the ground-state energy for r_s far beyond r_s^c as its calculation relies solely on the total charge-charge

structure factor $S_{CC}(q)$. A comparison among the results of ground-state energy at different ζ reveals, in qualitative agreement with the recent QMC studies,^{8,13} a continuous spin-polarization transition on increasing r_s , with the partially spin-polarized phases becoming stable over a definite range of r_s . As another interesting result, it is found that both the qSTLS and STLS methods underestimate the parallel spin-correlation energy while the antiparallel spin contribution is overestimated to the extent that the total correlation energy is in excellent agreement with the QMC data. We

believe that this result might be useful in further development of the theory of electron correlations.

ACKNOWLEDGMENTS

One of us (K.K.) acknowledges the financial assistance from CSIR, New Delhi, India. We also thank Giovanni B. Bachelet for providing us the FORTRAN codes of their analytical fits of the spin-resolved correlations.

*rkmoudgil13@gmail.com

- ¹See, for instance, G. D. Mahan, *Many-Particle Physics*, 2nd ed. (Plenum, New York, 1990); Gabriele F. Giuliani and Giovanni Vignale, *Quantum Theory of the Electron Liquid* (Cambridge University Press, New York, 2006).
- ²P. Hohenberg and W. Kohn, Phys. Rev. **136**, B864 (1964); W. Kohn and L. J. Sham, *ibid.* **140**, A1133 (1965); for review, see R. O. Jones and O. Gunnarsson, Rev. Mod. Phys. **61**, 689 (1989); W. Kohn, *ibid.* **71**, 1253 (1999).
- ³K. S. Singwi and M. P. Tosi, Solid State Phys. **36**, 177 (1981), and references therein.
- ⁴S. Ichimaru, Rev. Mod. Phys. **54**, 1017 (1982).
- ⁵N. H. March and M. P. Tosi, Adv. Phys. **44**, 299 (1995), and references therein.
- ⁶M. Hindgren and C.-O. Almbladh, Phys. Rev. B **56**, 12832 (1997) and references therein.
- ⁷D. P. Young, D. Hall, M. E. Torelli, Z. Fisk, J. L. Sarrao, J. D. Thompson, H.-R. Ott, S. B. Oseroff, R. G. Goodrich, and R. Zysler, Nature (London) **397**, 412 (1999).
- ⁸G. Ortiz, M. Harris, and P. Ballone, Phys. Rev. Lett. **82**, 5317 (1999); see also, W. E. Pickett and J. Q. Broughton, *ibid.* **48**, 14859 (1993).
- ⁹D. Ceperley, Phys. Rev. B **18**, 3126 (1978).
- ¹⁰D. M. Ceperley and B. J. Alder, Phys. Rev. Lett. **45**, 566 (1980).
- ¹¹G. Ortiz and P. Ballone, Phys. Rev. B **50**, 1391 (1994); **56**, 9970 (1997).
- ¹²Y. Kwon, D. M. Ceperley, and R. M. Martin, Phys. Rev. B **58**, 6800 (1998).
- ¹³F. H. Zong, C. Lin, and D. M. Ceperley, Phys. Rev. E **66**, 036703 (2002).
- ¹⁴C. Lin, F. H. Zong, and D. M. Ceperley, Phys. Rev. E **64**, 016702 (2001).
- ¹⁵F. Bloch, Z. Phys. **57**, 545 (1929).
- ¹⁶A. K. Rajagopal, S. P. Singhal, M. Banerjee, and J. C. Kimball, Phys. Rev. B **17**, 2262 (1978).
- ¹⁷S. Tanaka and S. Ichimaru, Phys. Rev. B **39**, 1036 (1989).
- ¹⁸P. Gori-Giorgi, F. Sacchetti, and G. B. Bachelet, Phys. Rev. B **61**, 7353 (2000).
- ¹⁹P. Gori-Giorgi and J. P. Perdew, Phys. Rev. B **66**, 165118 (2002).
- ²⁰P. Gori-Giorgi and J. P. Perdew, Phys. Rev. B **69**, 041103(R) (2004).
- ²¹B. Davoudi, R. Asgari, M. Polini, and M. P. Tosi, Phys. Rev. B **68**, 155112 (2003).
- ²²See, for instance, *Correlations in Electronic and Atomic Fluids*, edited by P. Jena, R. Kalia, P. Vashishta, and M. P. Tosi (World Scientific, Singapore, 1990), p. 5.
- ²³K. S. Singwi, M. P. Tosi, R. H. Land, and A. Sjölander, Phys. Rev. **176**, 589 (1968).
- ²⁴T. Hasegawa and M. Shimizu, J. Phys. Soc. Jpn. **38**, 965 (1975).
- ²⁵T. K. Ng and K. S. Singwi, Phys. Rev. B **35**, 6683 (1987).
- ²⁶J. Lindhard, K. Dan. Vidensk. Selsk. Mat. Fys. Medd. **28**, 8 (1954).
- ²⁷See for example, L. D. Landau and E. M. Lifshitz, *Statistical Physics*, 3rd ed. (Pergamon, New York, 1980), part 1.
- ²⁸See, for instance, D. Pines and P. Nozieres, *The Theory of Quantum Liquids* (Benjamin, New York, 1996), Vol. 1.
- ²⁹R. K. Moudgil, P. K. Ahluwalia, and K. N. Pathak, Phys. Rev. B **51**, 1575 (1995); **52**, 11945 (1995).
- ³⁰Vinayak Garg, R. K. Moudgil, Krishan Kumar, and P. K. Ahluwalia, Phys. Rev. B **78**, 045406 (2008).
- ³¹S. Moroni, D. M. Ceperley, and G. Senatore, Phys. Rev. Lett. **75**, 689 (1995).
- ³²R. Lobo, K. S. Singwi, and M. P. Tosi, Phys. Rev. **186**, 470 (1969).
- ³³T. Hasegawa and M. Shimizu, J. Phys. Soc. Jpn. **39**, 569 (1975).
- ³⁴E. Wigner, Phys. Rev. **40**, 749 (1932).